CEBAF PROPOSAL COVER SHEET

This Proposal must be mailed to:

CEBAF
Scientific Director's Office
12000 Jefferson Avenue
Newport News, VA 23606

and received on or before OCTOBER 30, 1989

A. TITLE: *The Electric Form Factor of the Neutron from the $d(\vec{e},e'\vec{n})p$ Reaction*

B. CONTACT PERSON: *Richard Madey*

ADDRESS, PHONE AND BITNET:

Physics Department
Kent State University
Kent, OH 44242

(216) 672-2596

BITNET: MADEV@KENTPHYS

C. THIS PROPOSAL IS BASED ON A PREVIOUSLY SUBMITTED LETTER OF INTENT

[X] YES *LOI-88-22*
[ ] NO

IF YES, TITLE OF PREVIOUSLY SUBMITTED LETTER OF INTENT

SAME

D. ATTACH A SEPARATE PAGE LISTING ALL COLLABORATION MEMBERS AND THEIR INSTITUTIONS

==========

(CEBAF USE ONLY)

Letter Received 10-30-89

Log Number Assigned PR-89-005

By KES

contact: Madey

RESEARCH PROPOSAL TO CEBAF

30 October 1989

THE ELECTRIC FORM FACTOR OF THE NEUTRON FROM THE $d(\vec{e},e'\vec{n})p$ REACTION

Scientific Participants

Richard Madey, Spokesman
B.D. Anderson
A.R. Baldwin
T. Eden
D. Keane
D.M. Manley
J. Schambach
J.W. Watson
W.M. Zhang
Graduate Students

Kent State University
Kent, Ohio 44242
(216) 672-2596

W. Bertozzi
S. Kowalski
C. Williamson

Massachusetts Institute of Technology
Cambridge, Massachusetts 02139

Bruce S. Flanders

The American University
Washington, D.C. 20016

P.J. Pella

Gettysburg College
Gettysburg, Pennsylvania 17325

Franz Gross
Jean Mougey
Paul Ulmer
Roy Whitney

CEBAF
Newport News, Virginia 23606

C.C. Chang
James J. Kelly

University of Maryland
College Park, Maryland 20742

J.M. Finn

College of William and Mary
Williamsburg, Virginia 23185

R. Lourie

University of Virginia
Charlottesville, Virginia 22904

THE ELECTRIC FORM FACTOR OF THE NEUTRON FROM THE $D(\vec{e},e'\vec{n})p$ REACTION

Abstract

We propose to determine the electric form factor G_E^n of the neutron by scattering longitudinally-polarized electrons from deuterium quasielastically and measuring the transverse polarization component $p_{S'}$ of the recoil neutron. The neutron polarization component $p_{S'}$, which lies in the scattering plane normal to the neutron momentum, is directly proportional to G_E^n in the impulse approximation. The neutron is detected in coincidence with the scattered electron. The experiment is based on a neutron polarimeter provided by Kent State University and a liquid-deuterium (LD) target capable of dissipating about 400 watts. A prototype (7 cm) LD target at MIT can handle an average beam current of 50 μA. Based on a (6/88) test run at Bates, the neutron polarimeter is expected to operate satisfactorily with a luminosity of 3×10^{38} $cm^{-2}s^{-1}$ at CEBAF.

The uncertainties in the best available measurements of G_E^n as a function of Q^2 are too large to distinguish between form factor models and not even between $G_E^n = 0$ and $G_E^n = -\tau G_M^n$ when the Dirac form factor $F_{1n} = 0$; however, the proposed experiment is designed to make these distinctions. The expected uncertainties ΔG_E^n are small fractions of the uncertainties in published data (from quasieleastic scattering of electrons from deuterium). Preliminary design considerations indicate that G_E^n can be measured as a function of Q^2, the four-momentum transfer squared, up to about 1.5 $(GeV/c)^2$ with a statistical uncertainty of $\pm$ 0.005 in the transverse polarization of the recoil neutron for four values of Q^2 in the range $0.30 \leq Q^2\ (GeV/c)^2 \leq 1.1$ and a statistical uncertainty of $\pm$0.010 for two additional points at Q^2 = 0.15 and 1.5 $(GeV/c)^2$. Except for the lowest Q^2 point, statistical uncertainties in the neutron polarization propagate to an uncertainty ΔG_E^n in G_E^n of typically $\pm$ 0.016 for $G_E^n = -\tau G_M^n$ and $\pm$ 0.01 or less for $G_E^n = 0$.

A theoretical study by Arenhövel (1987) indicates that the transverse polarization of the recoil neutron has almost no dependence on the deuteron model, and is insensitive to the influence of final-state interactions, meson-exchange currents, and isobar configurations.

THE ELECTRIC FORM FACTOR OF THE NEUTRON FROM THE $D(\vec{e},e'\vec{n})p$ REACTION

1. Scientific Background and Motivation

The electric form factor G_E^n of the neutron is a fundamental quantity needed for the understanding of both nucleon and nuclear structure. The dependence of G_E^n on Q^2, the four-momentum transfer squared, is determined by the charge distribution of the neutron. Also the Q^2-dependence of G_E^n tests the spatial symmetry of the neutron wave function under quark permutation. The electric form factor G_E^n is small and poorly known for all Q^2 except for the slope at $Q = 0$, which was obtained to 2% accuracy by scattering neutrons from atomic electrons [Krohn and Ringo (1966)]. Present models of the neutron predict different values of G_E^n at high momentum transfer; accordingly, good determinations of G_E^n will provide an important test of these models. Also the influence of G_E^n is not negligible in the interpretation of electron scattering from nuclei at high momentum transfer. For these reasons, it is of great importance to determine G_E^n with smaller uncertainties than before.

Our present knowledge of the electric and magnetic form factors G_E and G_M for protons and neutrons was obtained from measurements of the angular dependence of the cross section by elastic electron-proton scattering and quasielastic electron-deuteron scattering. The proton magnetic form factor G_M^p was extracted up to $Q^2 = 20$ $(GeV/c)^2$; and the neutron magnetic form factor G_M^n, up to $Q^2 = 10$ $(GeV/c)^2$.

Values of G_E^n obtained from measurements of <u>quasielastic</u> electron- deuteron scattering have large uncertainties. The values of G_E^n above $Q^2 = 0$ are consistent with zero; however, the uncertainties are too large to distinguish between different models or parameterizations such as $G_E^n = 0$ and $G_E^n = -\tau\, G_M$. We seek to determine values of G_E^n with uncertainties that are substantially smaller than the best published values, which were obtained by Bartel et al. (1973) from quasielastic electron-deuteron scattering, and that are free from the model dependencies (scale uncertainties) inherent in quasielastic electron-deuteron scattering. As shown in Fig. 1, the uncertainties projected from the proposed experiment will distinguish easily between $G_E^n = 0$ and the dipole parameterization $G_E^n = -\tau\, G_M$. At the Baltimore meeting of the American Physical Society, Platchkov (1989) reported new measurements from Saclay of the deuteron structure function $A(Q^2)$ up to $Q^2 = 18$ fm^{-2}. He claimed good accuracy (except for a scale factor) and inferred G_E^n up to 20 fm^{-2} [$= 0.78$ $(GeV/c)^2$] with the usual model dependencies inherent in quasielastic electron-deuteron scattering.

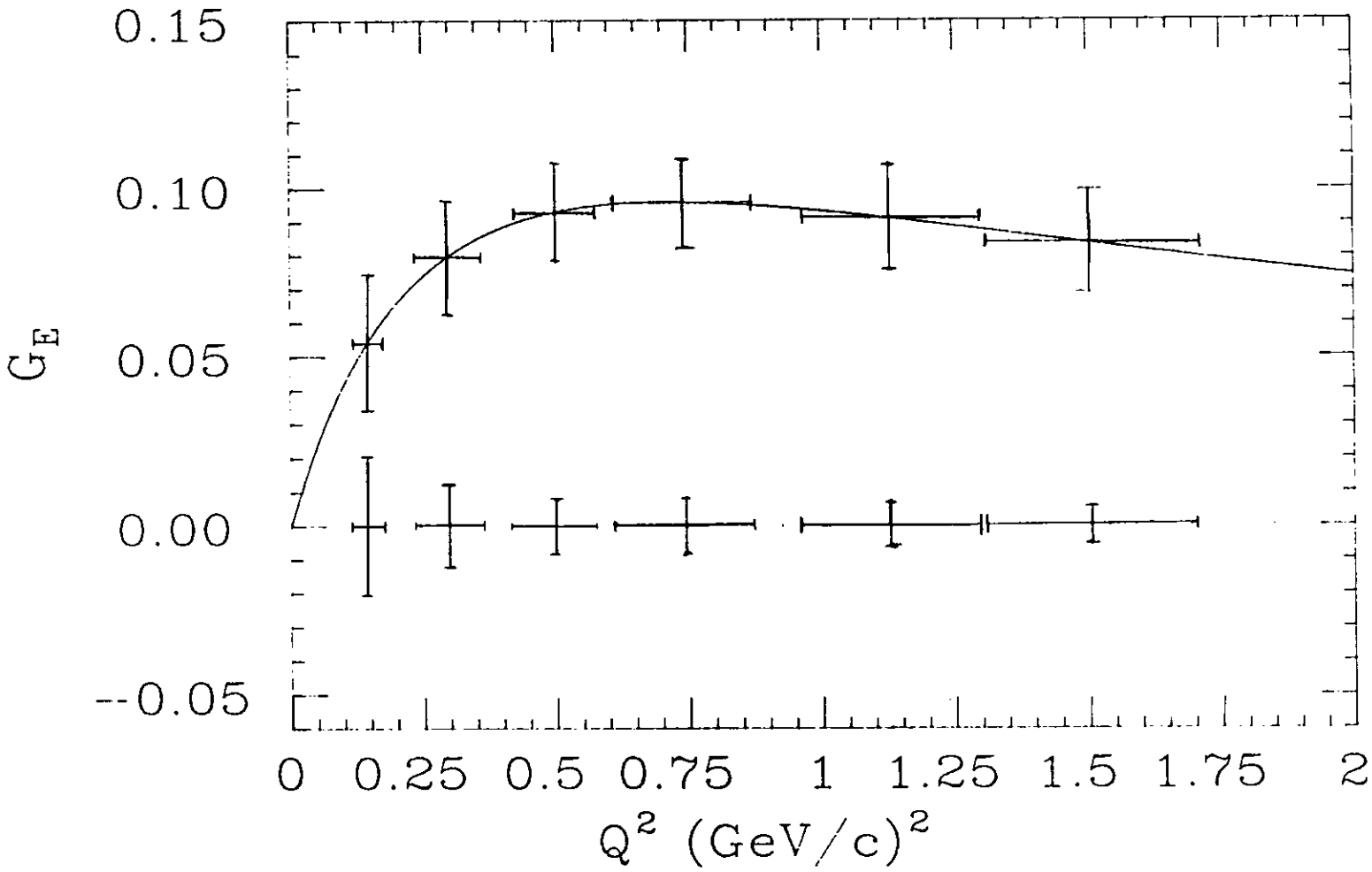

Fig. 1 Projected statistical uncertainties in G_E^n from the proposed experiment permit distinquishing between $G_E^n = 0$ and $G_E^n = \tau G_M^n$. (When the Dirac form factor $F_{1n} = 0$, $G_E^n = F_{1n} - \tau F_{2n} \Rightarrow -\tau G_M^n$.) This distinction is not possible with the best present data. The uncertainties shown here are based on a polarization uncertainty $\Delta p_{s'} = \pm 0.01$ for the two extreme points at $Q^2 = 0.15$ and 1.5 $(GeV/c)^2$ and $\Delta p_{s'} = \pm 0.005$ for the other four Q^2 points.

2. Measurement of G_E^n with a Neutron Polarimeter

Arnold, Carlson, and Gross (1981) suggested that G_E^n might be determined more accurately by measuring the polarization of the recoil neutron after quasielastic scattering of a longitudinally-polarized electron from an unpolarized neutron. The components of the polarization of the recoil neutron lie in the scattering plane of the electron and the recoil neutron. The polarization component normal to the scattering plane vanishes in the one-photon-exchange approximation. The component of the neutron polarization parallel to the scattering plane but normal to the momentum transfer is proportional to G_E^n. According to the Madison convention (1970), these nonzero components of the neutron polarization are $p_{S'}$ and $p_{L'}$, where L' denotes the direction of the path of the recoil neutron and, in a right-handed coordinate system, S' lies in the scattering plane.

The polarization transfer coefficient of special interest here is $D_{LS'}$ because it is related to G_E^n in the impulse approximation:

$$I_o\, D_{LS'} = -2\,(G_M^n\, G_E^n)[\tau\,(1+\tau)]^{\frac{1}{2}}\tan(\phi_e/2) \equiv -(G_M^n\, G_E^n)B(\phi_e,Q^2) \qquad (2.1)$$

with

$$I_o = (G_E^n)^2 + (G_M^n)^2\,\tau[1 + 2(1+\tau)\,\tan^2(\phi_e/2)] \approx A(\phi_e,Q^2)(G_M^n)^2 \qquad (2.2)$$

where $\tau = Q^2/4M^2$ and ϕ_e is the electron scattering angle. For the case of a longitudinally-polarized electron beam, $D_{LS'}$ is determined from the relation $p_{S'} = p_L D_{LS'}$ by measuring the neutron polarization $p_{S'}$ for a known (measured) longitudinal electron polarization p_L. Note that $D_{LS'} = p_{S'}$ for 100% polarization of the incident beam (i.e., for $p_L = 1$). The yield I_o is proportional to the double-scattering cross section (in units of the Mott cross section) with unpolarized electrons. Because $(G_E^n)^2$ can be neglected to give the right-hand-side of Eq. (2.2), the measurement of D_{LS} (or $p_{S'}$ and p_L) determines the ratio G_E^n/G_M^n:

$$\frac{G_E}{G_M} = D_{LS'}\,\frac{A(\phi_e,Q^2)}{B(\phi_e,Q^2)} = \frac{p_{S'}}{p_L}\,\frac{A(\phi_e,Q^2)}{B(\phi_e,Q^2)} \qquad (2.3)$$

Arnold, Carlson, and Gross (1981) calculated the recoil polarization $p_{S'}$ for various nucleon form factors. Plotted in Fig. 2 is the polarization

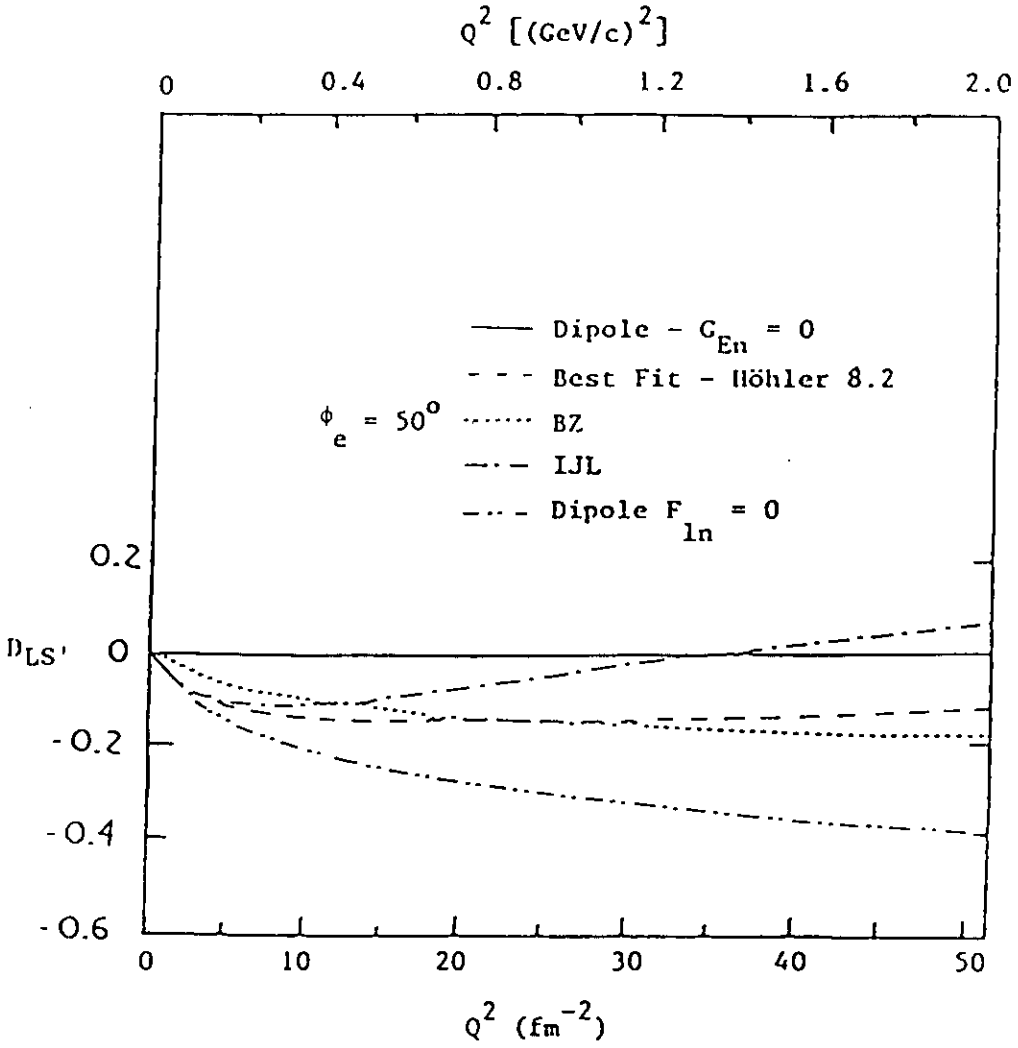

Fig. 2 The polarization transfer coefficient $D_{LS'}$ at an electron scattering angle ϕ_e = 50° calculated for various nucleon form factors as a function of Q^2, the four-momentum-transfer squared.

transfer coefficient $D_{LS'}$ at an electron scattering angle ϕ_e = 50° for several different form-factor models. All five models give plausible estimates for G_E^n within the range covered by the large uncertainties at the present time; however, these models predict large variations in the neutron polarization $p_{S'}$. As indicated later in this proposal, we are planning to measure the neutron polarization with an uncertainty that will be able to distinguish between some different models and particularly between $G_E^n = 0$ and the dipole parameterization $G_E^n = -\tau\ G_M^n$.

Arenhövel (1987) calculated the effect of the electric form factor of the neutron G_E^n on the polarization transfer in the $d(\vec{e},e'\vec{n})p$ reaction in the quasifree region, where the deuteron serves as a neutron target while the proton acts mainly as a spectator. Using a nonrelativistic theory and a realistic NN potential, he found that the polarization transfer coefficient $D_{LS'}$ (= $p_{S'}$ for P_L = 1), which vanishes for coplanar kinematics and unpolarized electrons, is most sensitive to G_E^n for neutron emission along the direction of the three-momentum transfer $\vec{q}$ in the quasifree case. Using the parametrization of Galster et al. (1971) for $G_E^n \neq 0$, he found that even away from the forward-emission direction with respect to the direction of the momentum transfer $\vec{q}$, the increase in $D_{LS'}$ by about 13% for $G_E^n \neq 0$ prevails up to a neutron angle ϕ_q of about 30°, measured with respect to the direction of the momentum transferred to the neutron by the electron. In the forward ($\phi_q \leq 30°$) direction with respect to $\vec{q}$, Arenhövel found also that the neutron polarization $p_{S'}$ is insensitive to the influence of final-state interactions, meson-exchange currents, and isobar configurations, and that this lack of sensitivity holds again up to an angle ϕ_q of 30° away from the forward direction with respect to $\vec{q}$. Finally, Arenhövel studied the influence of different deuteron wave functions on the polarization transfer coefficient $D_{LS'}$. His results for quasifree kinematics (i.e., for neutron emission along $\vec{q}$) show almost no dependence on the deuteron model. The Arenhövel calculation shows that dynamical uncertainties are very small.

3. Experimental Arrangement

In the proposed experiment, a longitudinally-polarized electron beam is incident on a liquid-deuterium target. The neutron polarimeter measures the transverse polarization $p_{S'}$ of the recoil neutron at a laboratory emission angle ϕ_n after quasielastic scattering of the longitudinally-polarized electron from an unpolarized neutron in deuterium. A magnetic spectrometer measures the momentum of the electron scattered at an angle ϕ_e. The recoil neutron is measured in coincidence with the scattered electron. The kinetic energy of the

neutron is obtained from a measurement of the neutron flight-time from the target to the front analyzing detectors in the polarimeter.

Based on measurements of neutrons in test runs at Bates in February and June 1988, the neutron polarimeter must be contained in a shielding enclosure similar to that shown in Fig. 3. The rear wall and the two side walls are concrete, four feet thick. The roof of the enclosure will be covered with concrete roof beams, two feet thick. The interaction mean free path in concrete for 75 MeV neutrons is about one foot; therefore, the transmission of 75 MeV neutrons through concrete is about 1.8% through four feet. The front wall consists of lead, 4 in. thick, supported by two steel plates, each 1 3/8 in. thick; in addition, steel (or concrete) blocks will be used to collimate the front detectors of the polarimeter and to provide additional shielding for the rear through this front wall shielding of 10.16 cm Pb plus 6.985 cm steel is 39 percent. The reduction in energy of a high-energy photon incident on this front shielding is 2.5×10^{-10}. Steel shadow shields, at least three feet thick, will be used to block the direct path of neutrons from the target in order to obtain a measure of the room background.

Shown in Fig. 4 is the configuration of the KSU neutron polarimeter. It consists of 12 scintillation detectors --- four primary scatterers (1 through 4) and two sets of four rear detectors. Rear detectors 5 through 8 are located at a mean scattering angle θ with respect to the direction of the incident neutrons; and rear detectors 9 through 12, at an angle minus θ. The positive and negative directions of the angle θ refer here to the positive and negative y' directions, respectively, in accordance with the Madison convention (1970). The mean flight path from the point midway between primary scatterers #2 and #3 to the midpoint of each rear detector array is 2.0 m. All 12 scintillation detectors are mounted with the long dimension normal to the plane of the paper. The rear detectors are 1.02 m long; the front detectors are 0.5 m long. The scintillators are 10 cm thick in the direction of the neutron flux. The primary scatterers are 25.4 cm high; the rear detectors are 50.8 cm high. In front of each set of four detectors is a thin (3/8 in.) plastic scintillation counter to veto charged particles. Additional information on this polarimeter is contained in an article by Madey et al (1989). This polarimeter was tested and calibrated in August 1989 with polarized neutrons of about 140 MeV from the Indiana University Cyclotron Facility. This polarimeter will be calibrated at neutron energies up to 800 MeV at LAMPF.

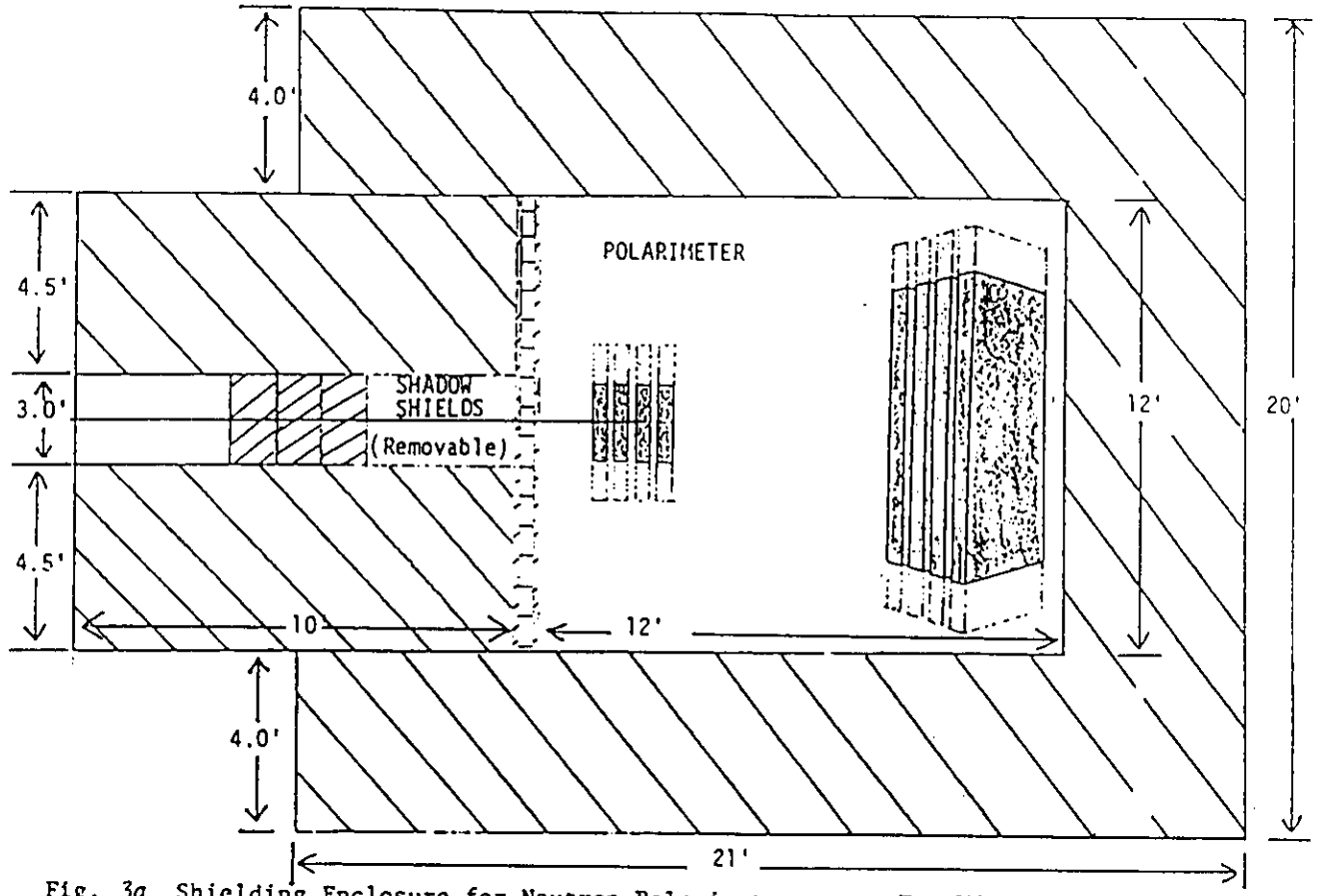

Fig. 3a Shielding Enclosure for Neutron Polarimeter - - - Top View

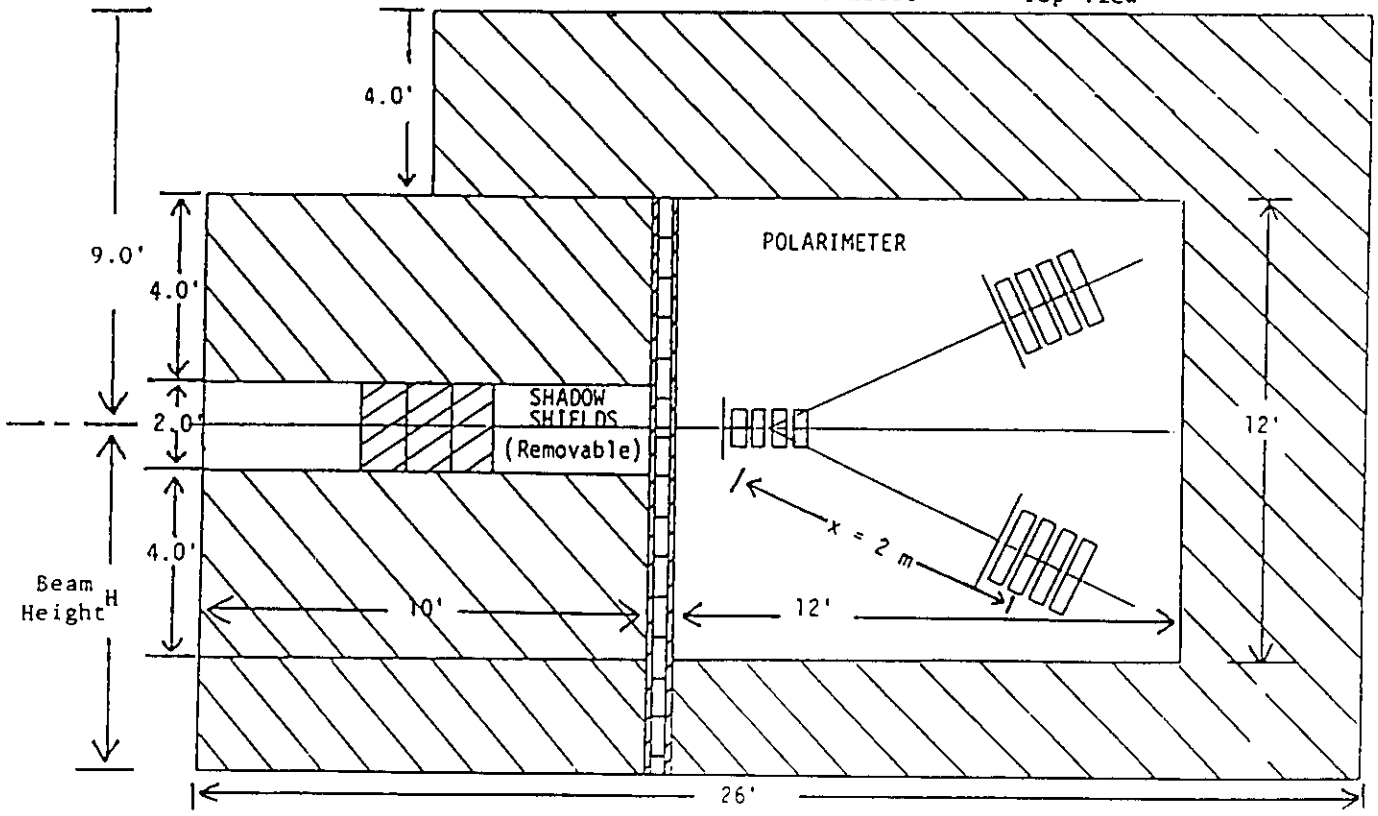

Fig. 3b Shielding Enclosure for Neutron Polarimeter - - - Side View

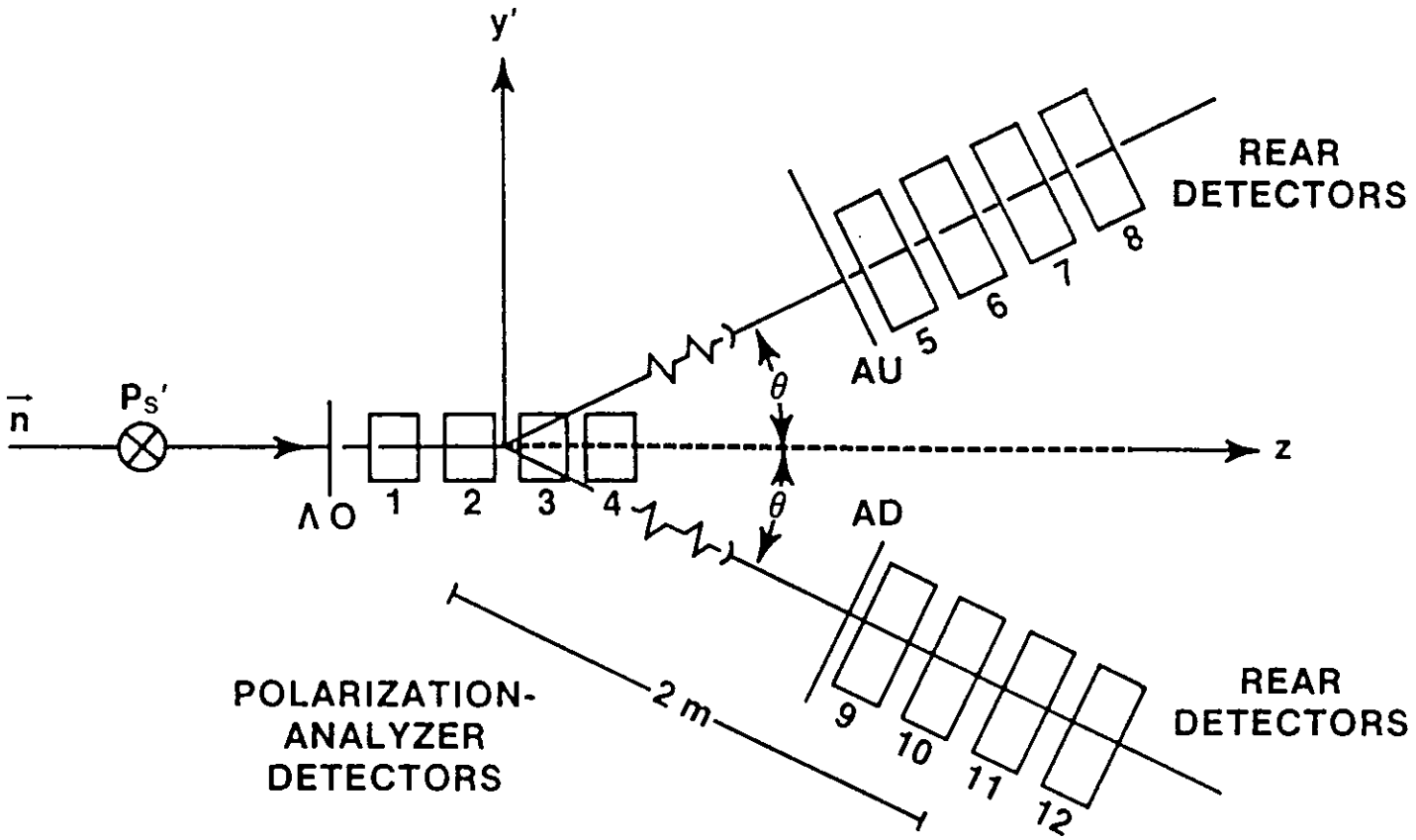

Fig. 4 Neutron polarimeter.

Because measurements of the neutron polarization will be made at different values of Q^2, the four-momentum-transfer squared, it is necessary to move the neutron polarimeter to neutron scattering angles ϕ_n that are matched kinematically to electron scattering angles ϕ_e; accordingly, to provide this capability, the neutron polarimeter together with its shielding should be mounted on a movable platform (e.g., air pads). The set of kinematic conditions in Table I illustrate the electron and neutron angles needed to make measurements of the neutron polarization for six values of Q^2 in the range $0.15 \leq Q^2(\mathrm{GeV/c})^2 \leq 1.5$.

4 Counting Rates

4.1 Solid-Angle Matching for e-n Coincidences

The polarization-analyzer detectors in the neutron polarimeter have a horizontal-to-vertical aspect ratio of two. In the normal operating mode, the magnet in the Hall A spectrometer has a vertical-to-horizontal aspect ratio of 2.17; the horizontal angular acceptance is ± 30 mr, and the vertical angular acceptance is ± 65 mr. The momentum acceptance of the Hall A magnet is ± 5 percent. In order to optimize the e-n coincidence rate, we want to provide the best match between the angular acceptances of the electron spectrometer and the angular acceptances of the neutron polarimeter.

The following notation corresponds to that in the TRANSPORT code where the Φ's are horizontal (i.e., transverse) angles and the Θ's are vertical (i.e., bend plane or dispersive) angles. For the case of elastic scattering from a stationary neutron, momentum conservation in the electron scattering plane (which may not be the horizontal plane) requires that

$$p_{e'} \sin \alpha = p_n \sin \beta \qquad (4.1.1)$$

For reactions that take place in the horizontal plane, (i.e., for vertical angles $\theta_e = \theta_n = 0$), the momentum conservation equation is

$$p_{e'} \sin \Phi_e = p_n \sin \Phi_n \qquad (4.1.2)$$

Table I. Kinematic Conditions for Measurements of the Neutron Polarization

Four Momentum-Transfer Squared	Incident Electron Energy	In-Plane Electron Angle	In-Plane Neutron Angle(i)	Scattered Electron Momentum	Neutron Kinetic Energy	Neutron Momentum	Neutron Horizontal Angular Interval(ii)	Electron Vertical Angular Inteval(iii)	Electron Solid Angle(ii)	Neutron Solid Angle(ii)	Electron Energy Bite(ii)
$Q^2 \pm \Delta Q^2$ $(GeV/c)^2$	E_e (GeV)	ϕ_e (deg)	$\phi_n + \Delta\phi_n$ (deg)	$p_{e'}$ (MeV/c)	T_n (MeV)	P_n (MeV/c)	$\Delta\phi_n$ (mr)	$\Delta\theta_e$ (mr)	$\Delta\Omega_e$ (msr)	$\Delta\Omega_n$ (msr)	$\Delta E_{e'}$ (MeV)
$1.498^{+0.207}_{-0.203}$	4.0	19.8	$47.54^{-2.60}_{+2.41}$	3200.7	797.6	1462.4	$\begin{matrix}-45.4\\ +42.1\\ \hline 87.5\end{matrix}$	11.61	1.38	4.44	218
$1.109^{+0.198}_{-0.190}$	4.0	16.5	$52.77^{-2.99}_{+2.79}$	3407.9	590.4	1208.5	$\begin{matrix}-52.2\\ -48.7\\ \hline 100.9\end{matrix}$	9.01	1.07	5.12	207
$0.747^{+0.125}_{-0.120}$	3.0	17.9	$56.60^{-2.60}_{+2.47}$	2600.7	397.6	952.3	$\begin{matrix}-43.1\\ +45.4\\ \hline 88.5\end{matrix}$	9.30	1.10	4.50	130
$0.500^{+0.067}_{-0.065}$	2.0	22.0	$58.66^{-2.05}_{+1.96}$	1732.2	266.1	756.4	$\begin{matrix}-35.8\\ +34.2\\ \hline 70.0\end{matrix}$	11.09	1.32	3.56	70.7
$0.299^{+0.059}_{-0.054}$	2.0	16.5	$65.52^{-2.27}_{+2.19}$	1839.0	159.3	570.5	$\begin{matrix}-39.6\\ +38.2\\ \hline 77.8\end{matrix}$	7.88	0.935	3.95	60.3
$0.149^{+0.026}_{-0.024}$	1.2	19.3	$68.63^{-1.72}_{+1.69}$	1118.8	79.5	395.1	$\begin{matrix}-30.0\\ +29.5\\ \hline 59.5\end{matrix}$	8.97	1.06	3.02	26.0

(i) For $\Delta\phi_e = \pm 1.70$ deg $= \pm 29.7$ mr

(ii) From kinematics

(iii) From momentum conservation $\left(\Delta\theta_e = \frac{p_n}{p_{e'}} \Delta\theta_n\right)$ and a neutron vertical angular acceptance $\Delta\theta_n = \pm 25.4$ mr (for a mean flight path x = 5.0 m).

Now for electron scattering planes that are rotated about the beam axis through a small angle θ with respect to the horizontal plane, momentum conservation relates the electron vertical angle θ_e to the neutron vertical angle θ_n:

$$p_{e'} \sin \theta_e = p_n \sin \theta_n \qquad (4.1.3)$$

The magnitude of the in-plane angular interval $\Delta\phi_n$ accepted by the neutron polarimeter depends on kinematics and on the magnitude of the in-plane angular acceptance $\Delta\phi_e$ for the coincident electrons. From the kinematics for the elastic n(e,e)n reaction, we obtain the results in Table I at selected values of Q^2, which are reached with different beam energies. For an electron horizontal angular acceptance $\Delta\phi_e = \pm 1.70^\circ = \pm 29.7$ mr, the associated neutron horizontal angular interval $\Delta\phi_n$ obtained from kinematics for the elastic n(e,e)n reaction is listed in Table I; for example, for $Q^2 = 0.747$ (GeV/c)^2, $\Delta\phi_n = \begin{matrix} -2.60^\circ \\ +2.47^\circ \end{matrix} = \begin{matrix} -43.1 \\ +45.4 \end{matrix}$ mr at 3.0 GeV. For a neutron flight path x from the target to a polarization-analyzer detector of height h, the neutron vertical angular acceptance $\Delta\theta_n$ is given by

$$\tan \Delta\theta_n = \frac{h/2}{x} \qquad (4.1.4)$$

For x = 5.0 m, $\Delta\theta_n = \pm 12.7$ cm/500 cm $= \pm 25.4$ mr.

The electron vertical angular interval $\Delta\theta_e$ that corresponds to the neutron vertical angular acceptance $\Delta\theta_n$ is obtained from the momentum conservation Eq. (4.1.3). From Table I for 3.0 GeV electrons scattered at $\phi_e = 17.9^\circ$, $p_n = 952.3$ MeV/c and $p_{e'} = 2600.7$ MeV/c; hence, for this case,

$$\Delta\theta_e = \frac{p_n}{p_{e'}} \Delta\theta_n = \left(\frac{952.3}{2600.7}\right) (\pm 25.4 \text{ mr}) = \pm 9.30 \text{ mr} \qquad (4.1.5)$$

The electron vertical angular acceptance $\Delta\theta_e$ ($= \pm 65$ mr) of the magnet in the Hall A spectrometer is much larger than necessary to accommodate $\Delta\theta_e = \pm 9.30$ mr. In order to reduce the singles counting rate in the electron arm, we plan to use a collimator to reduce the vertical angular acceptance $\Delta\theta_e$ to ± 12 mr. This vertical acceptance will accommodate the electron vertical angular intervals for all six Q^2 points proposed here, as can be seen in Table I.

The electron solid angle $\Delta\Omega_e$ is

$$\Delta\Omega_e = (2\Delta\theta_e)(2\Delta\phi_e) \qquad (4.1.6)$$

The neutron solid angle $\Delta\Omega_n$ is

$$\Delta\Omega_n = (2\Delta\theta_n)(2\Delta\phi_n) \qquad (4.1.7)$$

In order to estimate the real coincidence counting rates, we use electron and neutron solid angles that are correlated by kinematics. For an electron horizontal angular acceptance $\Delta\phi_e = \pm 1.70^\circ = \pm 29.7$ mr and a neutron vertical angular acceptance $\Delta\theta_n = \pm 25.4$ mr (at a mean flight path x = 5.0 m), the electron and neutron solid angles are obtained from elastic scattering of an electron from a free neutron at rest. The electron and neutron solid angles, which are obtained from two-body kinematics, are listed in Table I for each of the six Q^2 points; the neutron solid angle varies from about 3.6 to 5.1 msr, whereas the electron solid angle varies from about 0.94 to 1.4 msr.

Also listed in Table I for two-body kinematics is the full electron energy bite ΔE_e (MeV) that corresponds to the electron horizontal angular acceptance of ±29.7 mr.

In order to estimate the accidental coincidence counting rates, we calculate electron and neutron singles rates with solid angles based on the horizontal and vertical angular acceptances:

Electron horizontal angular acceptance,	$\Delta\phi_e$(mr) = ±29.7
Electron vertical angular acceptance, (from a collimator)	$\Delta\theta_e$(mr) = ±12.0
Electron solid angle,	$\Delta\Omega_e$(msr) = 1.42
Neutron horizontal angular acceptance,	$\Delta\phi_n$(mr) = ± 50.0
Neutron vertical angular acceptance,	$\Delta\theta_e$(mr) = ± 25.4
Neutron solid angle,	$\Delta\Omega_n$(msr) = 5.08

4.2 Coincidence Counting Rate

The electron-neutron coincidence counting rate R can be estimated from the following expression:

$$R = L\,\sigma(E_e, \phi_e, \phi_n)\,\Delta E_e\,\Delta\Omega_e\,\Delta\Omega_n\,\varepsilon_n\,\ell\,t \qquad (4.2.1)$$

where

$$\text{the luminosity } L(cm^{-2}s^{-1}) = F\,\rho_n x = F\rho x\,N_o/A \qquad (4.2.2)$$

and

F = incident flux of longitudinally-polarized electrons, electrons/s

ρ_n = numerical density of deuterium nuclei, cm^{-3}

ρx = thickness of liquid deuterium target,
= (0.169 g/cc) (5 cm) = 0.845 g/cm^2 ^2H

N_o = Avogadro's number (= 6.022×10^{23} nuclei/mole)

A = mass number of target (= 2.014 g/mole)

$\sigma(E_e,\phi_e,\phi_n)$ = triple differential cross section per deuterium nucleus for scattering an electron at an angle ϕ_e with an energy E_e in an interval ΔE_e and with a recoil neutron at an angle ϕ_n, $cm^2/MeV\cdot(sr)^2$ (The notation corresponds to that used in the transport code where ϕ's denote horizontal angles and θ's are vertical angles)

ΔE_e = width of the electron energy bite, MeV

$\Delta\Omega_e$ = electron solid angle

$\Delta\Omega_n$ = neutron solid angle

ε_n = efficiency of the neutron polarimeter

ℓ = live-time fraction of data acquisition system (~ 0.95)

t = transmission of neutrons from the target to the polarimeter through lead shielding designed to attenuate photons emitted from the target (t = 0.39 for 4 in. Pb contained within two 1 3/8 in. steel plates)

The experimental conditions for estimating the e-n coincidence counting rate for this experiment are listed in Table II. We used the plane-wave-impulse- approximation (PWIA) to calculate the triple-differential cross sections for the d(e,e'n)p reaction. As a test for the computer code [Manley (1987)], we checked the triple differential cross section calculated for the analogous d(e,e'p)n cross section at $\phi_e = 59^\circ$ at a bombarding energy of 500 MeV with that measured by Bernheim et al. (1981). The calculated

Table II Experimental Conditions for Counting Rate Estimates

1.	Beam	
1.1	Energy, E_e (GeV)	1.2,2.0,3.0,4.0 (See Table I)
1.2	Polarization, P_b	0.40 ± 0.02
1.3	Current, I(μA)	100, 25, 50
	Incident electron flux, $F(10^{14}e/s)$	6.2
1.4	Duty Factor	1.0
2.	Liquid Deuterium Target	
2.1	Thickness ρx[= (0.169 g/cm^3)(5.0 cm)]	0.845
2.2	Areal density of target nuclei, ρ_n x(deuts/cm^2)	2.53×10^{23}
3.	Luminosity, $F\ \rho_n x = L\ (10^{38}cm^{-2}s^{-1})$	1.6, 0.40, 0.80
4.	Neutron Polarimeter	
4.1	V-to-H aspect ratio, $\Delta\phi_n/\Delta\theta_n$	0.5
4.2	Mean flight path, x(m)	5.0
4.3	Vertical angular acceptance, $\Delta\theta_n$	$\pm$ 1.45° = $\pm$ 25.4 mr
4.4	Horizontal angular interval, $\Delta\phi_n$ (deg)	(See Table I)
4.5	Solid Angle, $\Delta\Omega_n$(msr)	(See Table I)
4.6	Efficiency, ε_n(%)	0.27
4.7	Average Analyzing Power, $\bar{A}_y$	0.38
4.8	Transmission of Neuts through Pb Shielding, t	0.39
4.9	Horizontal angular acceptance, $\Delta\phi_n$	$\pm$ 2.86 = $\pm$ 50 mr
4.10	Acceptance solid angle, $\Delta\Omega_n$(msr)	5.08
5.	Electron Spectrometer	
5.1	Horizontal angular acceptance, $\Delta\phi_e$	$\pm$ 1.70° = $\pm$ 29.7 mr
5.2	Vertical angular interval, $\Delta\theta_e$	$\pm$ 1.45° = $\pm$ 25.4 mr
5.3	Aspect ratio, $\Delta\phi_e/\Delta\theta_e$	1.2
5.4	Solid angle, $\Delta\Omega_e$ (msr)	(See Table I)
5.5	Energy acceptance, ΔE_e, (MeV)	(See Table I)
5.6	Vertical angular acceptance, $\Delta\phi_e$	$\pm$ 65 mr
5.7	Vertical angular acceptance, $\Delta\phi_e$ (mr) (after collimation)	$\pm$ 12 mr
5.8	Acceptance solid angle, $\Delta\Omega_e$ (msr)	1.42

cross sections are relatively insensitive to the assumed parameterization (e.g., $G_E = -\tau G_M$ or $G_E = 0$) of the neutron form factor. For the experimental conditions listed in Table II, the expression (4.2.1) for the electron-neutron coincidence counting rate becomes

$$R = (1.58 \times 10^{38}\,cm^{-2}s^{-1})(30 \times 10^{-33}\,cm^2/MeV\text{-}sr^2)(130\ MeV)(1.10 \times 10^{-3}\,sr)$$
$$\cdot(4.50 \times 10^{-3}\,sr)(0.27 \times 10^{-2})(0.95)(0.39) = 3.0\ s^{-1} \qquad (4.2.3)$$

The counting rate given by Eq. (4.2.3) will be an overestimate. To obtain a more realistic estimate, we must use the triple-differential cross section averaged over the experimental acceptances. To obtain this effective triple-differential cross section, we used the Monte Carlo code of P.E. Ulmer[1] to estimate the total number of electron events C_T expected in a specified data acquisition time (e.g., 3600 s) for the known differential cross section $d\sigma_{en}(\phi_e=17.9^\circ,\ E_e=3.0\ GeV)/d\Omega_e$ = 36 nb/sr. The Monte Carlo run, which takes into account the momentum distribution of the neutron in the deuteron, yields $C_T = 1.65 \times 10^4$ events in 3600 sec for the point at $Q^2 = 0.747\ (GeV/c)^2$ when the product of the luminosity ($L = 1.58 \times 10^{38}\ cm^{-2}s^{-1}$), the polarimeter efficiency ($\varepsilon = 0.27 \times 10^{-2}$), and the computer livetime ($\ell = 0.95$) is equal to $0.40 \times 10^{36}\ cm^{-2}s^{-1}$. This value of C_T implies that the effective triple differential cross section is

$$\frac{\overline{d^3\sigma}}{dE_e d\Omega_e d\Omega_n} = \frac{C_T}{\Delta\Omega_e \Delta\Omega_n \Delta E_e (\varepsilon_n L \ell) t(sec)} \qquad (4.2.4)$$

$$= \frac{1.65 \times 10^4}{(1.42\times10^{-3}\,sr)(5.08\times10^{-3}\,sr)(130)(0.40\times10^{36}\,cm^{-2}s^{-1})(3600\ s)} = 12\ nb/sr^2\ MeV$$

Thus, because the triple differential cross section averaged over the experimental acceptances is 40% of the quasielastic e-n cross section calcualted in the PWIA, the electron-neutron coincidence counting rate is 1.2 s^{-1}.

---

1 R.W. Lourie added an (e,e'n) option to P.E. Ulmer's (e,e'p) Monte Carlo code, called MCEEP.

The effective triple differential e-n cross sections $\overline{d^3\sigma}$ for the six Q^2 points are listed in Table III. Also listed in Table III are the PWIA triple differential cross sections $d^3\sigma$ for quasielastic e-n scattering, and the ratio $\overline{d^3\sigma}/d^3\sigma$. The real e-n coincidence counting rates $\bar{R}$ in Table III have taken into account the reduction factor $\overline{d^3\sigma}/d^3\sigma$.

4.3 Singles Counting Rates

Electron singles rates N_e are listed in Table III. These electron singles rates are based on double-differential cross sections calculated with the computer code of Dytmann (1987), which uses the equations of Moniz (1969). The singles counting rate N_e in the electron spectrometer can be estimated from the following expression:

$$N_e = L\ \sigma_2(\phi_e, E_e)\ \Delta E_e\ \Delta\Omega_e \qquad (4.3.1)$$

where

L = luminosity = $F(e/s)\ \rho_n x(d/cm^2)$

$\sigma_2(\phi_e, E_e')$ = double-differential cross section per deuterium nucleus for quasielastic scattering an electron at an angle ϕ_e with an energy E_e', $cm^2/MeV \cdot sr$ [$\sigma_2(\phi_e = 17.9, E_e' = 3.0$ GeV] = 1.4 nb/MeV-sr]

ΔE_e = width of the electron energy bite, [= 130 MeV from Table I]

$\Delta\Omega_e$ = acceptance solid-angle of the electron spectrometer, [= 1.42 msr from Table II]

The contribution to N_e from the Elgiloy (A=57) walls of the target is small compared to that from the deuterium because $L_{57}\sigma_{57} << L_2\sigma_2$. The expression for the average singles rate of electrons scattered at 17.9° by 3.0 GeV incident electrons yields the result that

$$N_e\ (e/s) = 4.1 \times 10^4. \qquad (4.3.2)$$

Electron singles rates for the other kinematic conditions are listed in Table III.

Table III. Counting Rates and Data Acquisition Times

I (μA)	E_e (GeV)	Q^2 $(GeV/c)^2$	Electron Singles Rate N_e $(10^4 e/s)$	Neutron Singles Rates $(10^2$ n/s) N_n^D	N_n^W	N_n^C	N_n	Coincidence Rates (s^{-1}) A	R	$\bar{R}$	$\bar{R}/A$	Required Events(i) $10^{-4}N$	Aquisition Time T=N/R (hr)	Cross Sections $(nb/sr^2\text{-MeV})$ $d^3\sigma$	$\bar{d^3\sigma}$	$\bar{d^3\sigma}/d^3\sigma$
25	1.2	0.149	9.3	2.5	0.43	2.8	5.8	0.18	0.43	0.38	2.1	12.5	94	130	114	0.88
50	2.0	0.299	13.5	5.1	0.86	11	17	0.8	2.15	1.2	1.5	48	116	120	65	0.54
100	2.0	0.500	4.7	10.2	1.7	46	57	0.92	2.0	1.2	1.3	53.0	115	39	23	0.58
100	3.0	0.747	4.1	10.2	1.7	46	57	0.79	3.1	1.2	1.5	42.2	78	30	12	0.40
100	4.0	1.11	2.0	10.2	1.7	46	57	0.39	2.3	0.80	2.0	37.3	130	13	4.6	0.35
100	4.0	1.50	0.47	10.2	1.7	46	57	0.091	0.60	0.35	3.8	9.0	72	2.9	1.7	0.58
												605				

(i) For Q^2 = 0.15 and 1.5 $(GeV/c)^2$, $\Delta p_{s'} = \pm 0.010$; for the other four Q^2 points, $\Delta p_{s'} = \pm 0.005$.

The singles counting rates in the neutron polarimeter were estimated on the basis of the results from a (6/13/88) test run at Bates with 762 MeV incident electrons that the neutron flux at 56.6° is about 2.2 x 10^3 n/s-μA-msr-g-cm^{-2} from a deuterium target and about 4.4 x 10^3 n/s-μA-msr-g-cm^{-2} from an Elgiloy target. The measured neutron emission rates from both deuterium and Elgiloy agree reasonably well with those expected from cross sections. The calculated rate from deuterium is about 30% smaller at 1.5 x 10^3 n/s-μA-msr-g-cm^{-2} $^2_1$H; that from Elgiloy is about 5% smaller at 4.2 x 10^3 n/s-μA-msr-g-cm^{-2} ^{57}Fe. The neutron flux observed from deuterium is about the same as that measured by Barreau et al (1980) at Saclay at a beam energy of 500 MeV; whereas the flux of background neutrons from Elgiloy at 762 MeV is about one-fourth of the Saclay result from stainless steel at 500 MeV. The shielded neutron detectors operated satisfactorily at a luminosity of 3x10^{36} cm^{-2} s^{-1} with a Bates duty factor of 1%. The limitation on the luminosity comes from chance coincidences between the front and rear detectors of the polarimeter. Neutron singles rates N_n are listed in Table III for the six Q^2 points proposed here (see Section 4.4 also).

4.4 Accidental Coincidence Counting Rates

The accidental coincidence counting rate beneath the peak of the real electron-neutron coincidence counting rate is given by

$$A = \frac{\tau}{f} N_e \; N_n \qquad (4.4.1)$$

where f is the duty factor of the accelerator, τ is the width of the peak, N_e is the counting rate in the electron spectrometer, and N_n is the counting rate in the neutron polarimeter. Contributions to N_n come from the deuterium in the target cell (N_n^D), the walls of the target cell (N_n^W), and chance coincidences (N_n^C) between an event in a front detector and an event in a rear detector of the polarimeter; that is,

$$N_n = N_n^D + N_n^W + N_n^C. \qquad (4.4.2)$$

The rates N_n^D, N_n^W, and the chance coincidence rates N_n^C between front and rear detectors in the polarimeter were measured in the (6/12/88) test run at Bates and scaled appropriately for the conditions of the proposed experiment. Contributions to N_n^C come from the deuterium in the target cell and the walls of the target cell; that is,

$$N_n^C = (N_n^C)_D + (N_n^C)_W \qquad (4.4.3)$$

The counting rate in the neutron polarimeter can be written as follows:

$$N_n = (rI + aI^2)\Delta\Omega_n = (r_2 + r_{57})\Delta\Omega_n\, I + (a_2 + a_{57})\Delta\Omega_n\, I^2 \qquad (4.4.4)$$

where $r_{2(57)}$ and $a_{2(57)}$ are the real and accidental counting rates, respectively, of neutrons from deuterium (Elgiloy) per unit neutron solid angle and per unit beam current. We obtained values for the real coefficients from the normalized yields observed in our (6/12/88) test run at Bates. The normalized neutron yields from the target are as follows:

$$Y_2 = 2.2 \times 10^3 \text{ n/s-}\mu\text{A-msr-g-cm}^{-2}\ {}^2_1\text{H} \qquad (4.4.5)$$

$$Y_{57} = 4.4 \times 10^3 \text{ n/s-}\mu\text{A-msr-g-cm}^{-2}\ \text{Elgiloy} \qquad (4.4.6)$$

Thus, for a deuterium target thicknesses of 5 cm (= 0.845 g/cm^2 ${}^2_1$H) and for two 2-mil-thick Elgiloy walls (x_{57} = 0.080 g/cm^2 Elgiloy), the real coefficients are as follows:

$$r_2 \ (\text{n/s-msr-}\mu\text{A}) = 2.0 \qquad (4.4.7)$$

$$r_{57} \ (\text{n/s-msr-}\mu\text{A}) = 0.34 \qquad (4.4.8)$$

$$r = r_2 + r_{57} = 2.34 \qquad (4.4.9)$$

Thus, for I = 100 μA and $\Delta\Omega_n$ = 5.08 msr (from the neutron angular acceptances), the real counting rate of neutrons in the polarimeter from 0.845 g/cm^2 ${}^2_1$H and from 0.080 g/cm^2 Elgiloy (for a polarimeter efficiency $\epsilon = 0.27 \times 10^{-2}$ and a neutron transmission through the front shielding wall t = 0.39) are

$$N_n^D = 1016 \text{ s}^{-1} \qquad (\epsilon = 0.27\text{x}10^{-2};\ t = 0.39) \qquad (4.4.10)$$

$$N_n^W = 173 \text{ s}^{-1} \qquad (\epsilon = 0.27\text{x}10^{-2};\ t = 0.39) \qquad (4.4.11)$$

$$N_n^R = N_n^D + N_n^W = 1189 \text{ s}^{-1} \qquad (4.4.12)$$

For the two-detector prototype polarimeter in the (6/88) test run at Bates, the background counting rate $(N_n^C)_W$ is 1.37 sec^{-1} from the 0.2 g/cm^2 Elgiloy walls at an average beam current of 0.98 μA, and $(N_n^C)_{D+W}$ is 19.8 sec^{-1} from the

10 cm liquid deuterium in the target cell plus the 0.2 g/cm^2 Elgiloy walls of the cell at an average beam current of 0.93 μA. These rates were measured for a neutron transmission t = 0.26. The background counting rates from the deuterium and from the walls scale with the square of the luminosity; accordingly, for I = 0.93 μA, $(N_n^C)_W$ = 1.23 s^{-1} and $(N_n^C)_D = (N_n^C)_{D+W} - (N_n^C)_W$ = 19.8 - 1.2 = 18.6 s^{-1}. Also the background counting rates are assumed to scale linearly with the neutron transmission and with the neutron solid angle subtended by a front detector. Because the rear detector was shielded heavily by an additional three feet of steel between it and the target, the singles rate in the rear detector comes primarily from room background; accordingly, this rate is insensitive to relatively small changes in the position of the rear detector with respect to the target. In the proposed experiment, the background rates must be multiplied by a factor of 11 to account for the increase in the efficiency of the full-scale (12-detector) polarimeter with mineral-oil front detectors over the prototype polarimeter with two NE-102 plastic scintillators. Thus,

$$N_n^C = \left(N_n^C\right)_D + \left(N_n^C\right)_W \tag{4.4.13}$$

$$\left(N_n^C\right)_D = (18.6\ s^{-1})(11)\left(\frac{t}{0.26}\right)\left(\frac{\Delta\Omega_n(msr)}{10.3\ msr}\right)\left[\left(\frac{I(\mu A)}{0.93\ \mu A}\right)\left(\frac{x(cm)}{10\ cm}\right)\right]^2\left(\frac{0.01}{f}\right) \tag{4.4.14}$$

$$\left(N_n^C\right)_W = (1.37\ s^{-1})(11)\left(\frac{t}{0.26}\right)\left(\frac{\Delta\Omega_n(msr)}{10.3\ msr}\right)\left[\left(\frac{I(\mu A)}{0.98\ \mu A}\right)\left(\frac{\rho x(g/cm^2)}{0.2\ g/cm^2}\right)\right]^2\left(\frac{0.01}{f}\right) \tag{4.4.15}$$

Thus, for a deuterium target thickness x_2 = 5 cm ^2_1H and for two 2-mil-thick Elgiloy walls (x_{57} = 0.080 g/cm^2), the accidental coefficients a_2 and a_{57} are:

$$a_2(n/s\text{-}msr\text{-}\mu A^2) = 8.6\ (0.01/f) = 8.6x10^{-2} \qquad (t=0.39;\ \epsilon=0.27x10^{-2}) \tag{4.4.16}$$

$$a_{57}(n/s\text{-}msr\text{-}\mu A^2) = 0.36\ (0.01/f) = 0.36x10^{-2} \qquad (t=0.39;\ \epsilon=0.27x10^{-2}) \tag{4.4.17}$$

$$a_2 + a_{57} = 8.96 \times 10^{-2} \qquad (t=0.39;\ \epsilon=0.27x10^{-2}) \tag{4.4.18}$$

The right-hand equalities are for CEBAF with f=1.0. Thus, for I=100 μA and $\Delta\Omega_n$ = 5.08 msr, the accidental counting rate of neutrons between front and rear detectors in the polarimter (with an efficiency ϵ = 0.27 x 10^{-2} and a neutron transmission t=0.39 are:

$$N_n^C=(N_n^C)_D+(N_n^C)_W=(8.96x10^{-2}\ n/s\text{-}msr\text{-}\mu A^2)(5.08\ msr)(100\mu A)^2=4.55x10^3\ n/s \tag{4.4.19}$$

The sum of N_n^C and N_n^R [from Eq. (4.4.12)] is

$$N_n(s^{-1}) = N_n^C + N_n^R = 4550 + 1189 = 5739 \qquad (4.4.20)$$

Neutron singles rates are listed in Table III for the six Q^2 points proposed here.

Finally, for τ = 3.4 ns (fwhm) and $N_e = 4.1 \times 10^4$ e/s for the point at Q^2 = 0.747 $(GeV/c)^2$, the accidental coincidence rate is

$$A(s^{-1}) = (3.4 \times 10^{-9}s)(4.1 \times 10^4 e/s)(5.7 \times 10^3\ n/s) = 0.79 \qquad (4.4.21)$$

Accidental coincidence rates are listed in Table III for the six Q^2 points proposed here. The ratio of the real-to-chance coincidence counting rates for the point at Q^2 = 0.747 $(GeV/c)^2$ is expected to be

$$\bar{r} \equiv \frac{\bar{R}}{A} = \frac{1.2}{0.55} = 1.5 \qquad (4.4.22)$$

These ratios are listed in Table III for the six Q^2 points proposed here.

5. Statistics and Uncertainties

The number of events N needed to measure the neutron polarization $p_{s'}$ with a specified uncertainty $\Delta p_{s'}$ is given, to a good approximation, by

$$N = \frac{(1+2/\bar{r})}{(\bar{A}_y \Delta p_{s'})^2} \qquad \bar{r} \equiv \bar{R}/A \qquad (5.1)$$

where $\bar{A}_y$ is the average analyzing power of the polarimeter, and $\bar{r}$P@B($\equiv\bar{R}/A$) is the ratio of the real events $\bar{R}$ to the accidental events A. For $\bar{A}_y$ = 0.38, the number of events to achieve polarization uncertainties $\Delta p_{s'} = \pm 0.010$ and $\Delta p_{s'} = \pm 0.005$ are

$$N = 6.93 \times 10^4(1+2/\bar{r}) \quad (\text{for } \Delta p_{s'} = \pm 0.010) \qquad (5.2a)$$

$$N = 27.7 \times 10^4(1+2/\bar{r}) \quad (\text{for } \Delta p_{s'} = \pm 0.005) \qquad (5.2b)$$

Values of N are listed in Table III for the six Q^2 points proposed here. Also listed in Table III are data acquisition times to acquire this number of events.

From Eq. (2.3), the relative uncertainty in the ratio G_E^n/G_M^n is:

$$\frac{\Delta(G_E^n/G_M^n)}{(G_E^n/G_M^n)} = \left[\left(\frac{\Delta p_{S'}}{p_{S'}}\right)^2 + \left(\frac{\Delta p_L}{p_L}\right)^2 + \left(\frac{1}{A}\frac{\partial A}{\partial \phi_e} - \frac{1}{B}\frac{\partial B}{\partial \phi}\right)^2 (\Delta\phi)^2 - \left(\frac{1}{A}\frac{\partial A}{\partial Q^2} - \frac{1}{B}\frac{\partial B}{\partial Q^2}\right)^2 (\Delta Q^2)^2\right]^{\frac{1}{2}} \quad (5.3)$$

Case I: For $G_E^n = 0$, $\Delta G_E^n = G_M^n \Delta (G_E^n/G_M^n)$ (5.4)

For the case $G_E^n = 0$, the evaluation of the uncertainty $\Delta(G_E/G_M)$ in Eq. (5.3) simplifies because multiplication of both sides of Eq. (5.3) by G_E^n/G_M^n causes all terms to vanish except the term with $\Delta p_{S'}$:

$$\Delta\left(\frac{G_E^n}{G_M^n}\right) = \left(\frac{G_E^n}{G_M^n}\right)\left(\frac{\Delta p_{S'}}{p_{S'}}\right) = \frac{A(\theta_e, Q^2)}{B(\theta_e, Q^2)}\frac{\Delta p_{S'}}{p_L} \quad (5.5)$$

The right-hand member follows from Eq. (2.3). Listed in Table IV for the six Q^2 points proposed here are the values of the ratio $A(\phi_e, Q^2)/B(\phi_e, Q^2)$, and the uncertainty in the ratio G_E^n/G_M^n for $p_L = 0.40$ and $\Delta p_{S'} = 0.010$ for the points at $Q^2 = 0.149$ and 1.498 $(GeV/c)^2$ and $\Delta p_{S'} = 0.005$ for the other four Q^2 points. Also listed in Table IV are the expected uncertainties in G_E^n with values of the magnetic form factor G_M^n based on the parameterization

$$G_M^n = (-1.91)/(1 + Q^2/0.71)^2 \quad (5.6)$$

The expected uncertainties ΔG_E^n listed in Table IV are about 0.01 or less for the five higher Q^2 points and 0.02 for the lowest Q^2 point.

Case II: For $G_E^n = -\tau G_M^n$ with $G_E^n = (-1.91)/(1+Q^2/0.71)^2$

For this dipole parameterization, the values of G_E^n and the associated values of $p_{S'}$ from Eq. (2.3) are listed in Table V for the six Q^2 points proposed here.

Because $\epsilon = p_{S'}\bar{A}_y$, the relative uncertainty $(\Delta p_{S'}/p_{S'})$ is:

$$\left(\frac{\Delta p_{S'}}{p_{S'}}\right)^2 = \left(\frac{\Delta\epsilon}{\epsilon}\right)^2 + \left(\frac{\Delta\bar{A}_y}{\bar{A}_y}\right)^2 = \frac{1-2A/R}{\epsilon^2 N} + \left(\frac{\Delta\bar{A}_y}{\bar{A}_y}\right)^2 \quad (5.7)$$

The right-hand member follows from the fact the $\Delta\epsilon = (1+2A/R)^{1/2}/N^{1/2}$. The factor $1/N^{1/2}$ comes from a binomial distribution for N_u events. The factor $(1+2A/R)^{1/2}$ comes from subtraction of A accidental events from the R real plus A

Table IV Expected Uncertainties ΔG_E^n if $G_E^n = 0$

E_e (GeV)	Q^2 $(GeV/c)^2$	ϕ_e (deg)	A/B	$\Delta(G_E^n/G_M^n)$	$-G_M^n$	ΔG_E^n	$\Delta p_s'$
1.2	0.149	19.3	0.63	0.016	1.30	0.021	0.010
2.0	0.299	16.5	1.00	0.013	0.95	0.012	0.005
2.0	0.500	22.0	0.98	0.012	0.66	0.0081	0.005
3.0	0.747	17.9	1.41	0.018	0.45	0.0080	0.005
4.0	1.109	16.5	1.78	0.022	0.29	0.0065	0.005
4.0	1.498	19.8	1.70	0.042	0.20	0.0084	0.010

Table V Expected Uncertainties ΔG_E^n if $G_E^n = -\tau G_M^n$

E_e (GeV)	Q^2 $(GeV/c)^2$	ϕ_e (deg)	G_E^n	p_s'	$\Delta p_s'/p_s'$ (Note 1)	$\frac{\Delta(G_E^n/G_M^n)}{G_E^n/G_M^n}$	$\Delta G_M^n/G_M^n$ (Note 2)	$\Delta G_E^n/G_E^n$	ΔG_E^n	$G_E^2 \pm \Delta G_E^2$ (Note 3)	$\Delta p_s'$
1.2	0.149	19.3	0.055	0.027	0.38	0.39	0.1	0.40	0.022		0.010
2.0	0.299	16.5	0.080	0.034	0.15	0.19	0.1	0.21	0.017		0.005
2.0	0.500	22.0	0.093	0.058	0.094	0.13	0.1	0.16	0.015	-0.004 ± 0.006	0.005
3.0	0.747	17.9	0.096	0.060	0.091	0.14	0.1	0.17	0.016	0.0058 ± 0.0077	0.005
4.0	1.109	16.5	0.091	0.071	0.080	0.14	0.1	0.17	0.016	0.0013 ± 0.007	0.005
4.0	1.498	19.8	0.084	0.10	0.11	0.14	0.1	0.18	0.015	0.0021 ± 0.0025	0.010

Note 1: The contributions from the other three terms in Eq. (5.1) are small

Note 2: From Hughes et al (1965) for $Q^2 < 0.75$ $(GeV/c)^2$. For $Q^2 \geq 0.75$ $(GeV/c)^2$, the present relative uncertainties $\Delta G_M/G_M$ are larger than the assumed value of 0.1. New measurements of G_M^n are needed for $Q^2 \geq 0.75$ $(GeV/c)^2$ to reduce the relative uncertainties in $\Delta G_M/G_M$ to values ≤ 0.1.

Note 3: From Bartel et al (1973)

accidental events. Values of $(\Delta p_{S'}/p_{S'})$ from Eq. (5.7) and values of $\Delta(G_E^n/G_M^n)/(G_E^n/G_M^n)$ from Eq. (5.3) are listed in Table V for the six Q^2 points proposed here. The relative uncertainty in G_E^n depends on the relative uncertainty in G_M^n:

$$\frac{\Delta G_E}{G_E^n} = \left[\left(\frac{\Delta(G_E/G_M)}{G_E^n/G_M^n}\right)^2 + \left(\frac{\Delta G_M}{G_M^n}\right)^2\right]^{1/2} \tag{5.8}$$

For a relative uncertainty $\Delta G_M^n/G_M^n = 0.1$, the expected uncertainties ΔG_E^n are listed in Table V and plotted in Fig. 1 for this dipole parameterization of G_E^n. The relative uncertainties in $\Delta G_M^n/G_M^n = 0.1$ are consistent with the data of Hughes et al (1965) for the three lowest Q^2 points; however, the data of Hughes et al. have higher relative uncertainties $\Delta G_M^n/G_M^n \sim 0.2$ for $Q^2 \gtrsim 0.75$ $(GeV/c)^2$. New measurements of G_M^n are needed to reduce the relative uncertaintiy $\Delta G_M^n/G_M^n$ to values less than 0.1.

For the point at $Q^2 = 0.500$ $(GeV/c)^2$, we plot as a function of $p_{S'}$ in Fig. 5 the value of $G_E^n \pm \Delta G_E^n$ that we would expect to obtain from a measurement of the unknown value of $p_{S'}$ for a beam polarization $p_L = 0.4$ and an average analyzing power $\bar{A}_y = 0.38$.

6. Beam Time Request

The beam-time request for measurements of G_E^n at six Q^2 points from about 0.15 to 1.5 $(GeV/c)^2$ is as follows:

	Beam on Target (Hours)
Tuneup and checks of electron spectrometer	24
Checkout of neutron polarimeter and tests of e-n coincidences	24
Data acquisition -- target in	605
Data acquisition -- dummy target cell	100
Electron beam polarization measurements	76
Overhead (~10%) (Reversal of direction of beam polarization, checking liquid deuterium target, insertion and removal of targets, pulse-height calibrations of polarimeter detectors, stopping and restarting data acquisition system, ...)	81
	910

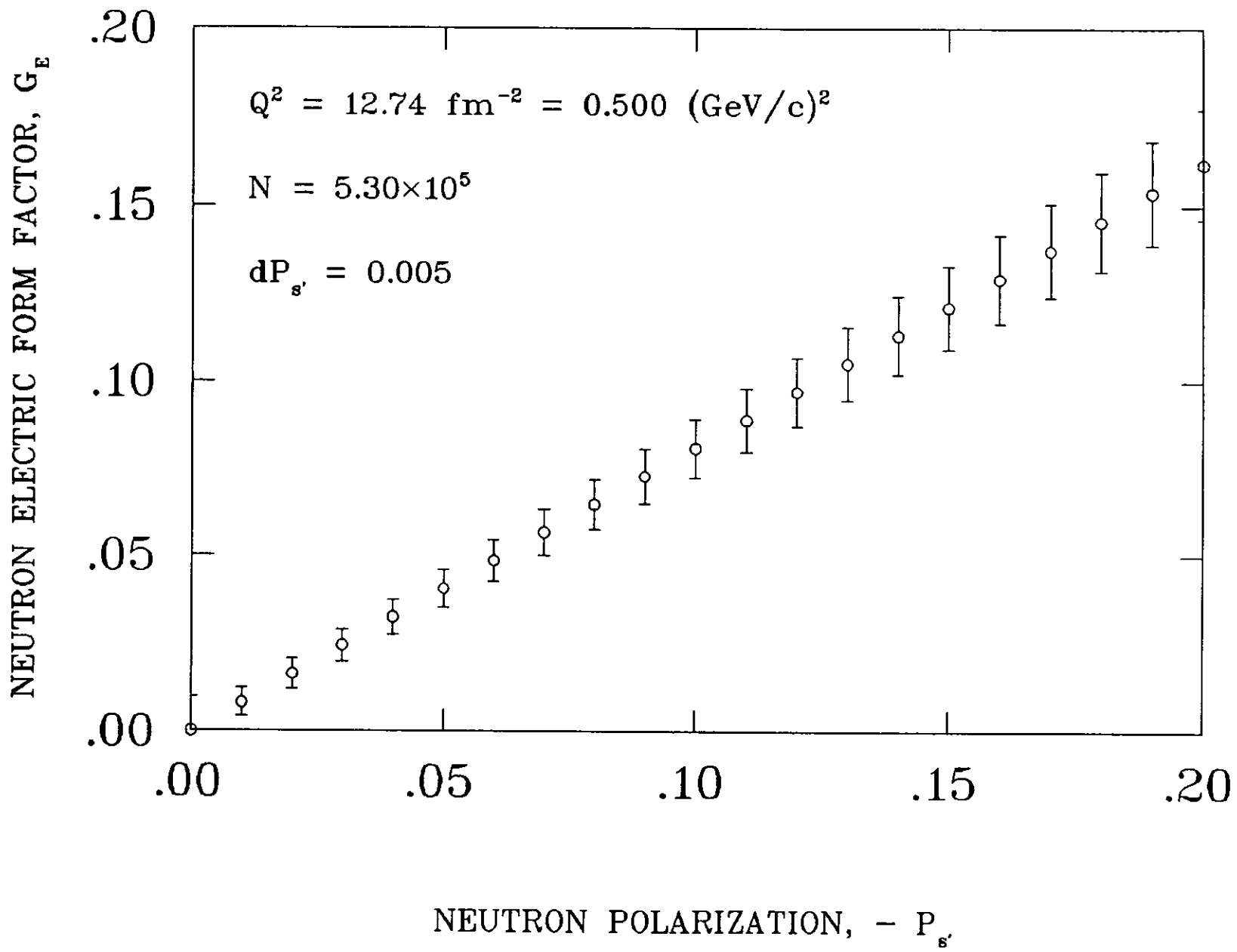
NEUTRON ELECTRIC FORM FACTOR, G_E
.20
.15
.10
.05
.00
Q^2 = 12.74 fm^{-2} = 0.500 $(GeV/c)^2$
N = 5.30×10^5
$dP_{s'}$ = 0.005
.00
.05
.10
.15
.20
NEUTRON POLARIZATION, $- P_{s'}$

7. Collaboration

The scientific participants in this collaboration have been involved in the same experiment to measure G_E^n at one value of Q^2 at Bates. This experiment will constitute an effort of the highest priority for the Kent State group. Kent State personnel will be involved in all aspects of the experiment, will provide the neutron polarimeter and be responsible for its operation, and will provide dissertation students for this research. Kent State University will provide the data acquisition program. The liquid deuterium target will be the joint responsibility of personnel from MIT and CEBAF. Personnel from William and Mary, Maryland, Virginia, and CEBAF will be responsible for the operation of the electron spectrometer. Roy Whitney will spearhead the development of detectors for the electron spectrometer.

Dr. F. Gross (CEBAF) will be concerned primarily with the theoretical interpretation of the data. Fully relativistic calculations will extend the non-relativistic treatment of Arenhövel (1987). These relativistic calculations should work extremely well at the quasielastic peak and over the Q^2 range proposed for this experiment. This theoretical work is expected to be complete long before this experiment is carried out, and all theoretical uncertainties are expected to be smaller than the experimental errors.

Needed from CEBAF to do this experiment is a longitudinally-polarized electron beam, a liquid-deuterium target, and shielding for the neutron polarimeter. The neutron polarimeter together with its shielding should be on a movable platform in order to change the neutron scattering angles.

Note that the requirements for an electron spectrometer for this experiment can be met by magnets in either Hall A or Hall C; accordingly, because this collaboration is interested in running this experiment during the first phase of experimental operations at CEBAF, we are interested in mounting this experiment in the first experimental hall that will be ready to accept this experiment.

8. References

ARENHOVEL, H. Phys. Lett. B. 199, 13 (1987).

ARNOLD, R.G. and C.E. Carlson and F. Gross, Phys. Rev C23, 363 (1981).

BARREAU, P., Status Report on the Study of Feasibility of the (e,e'n) Reactions in the HE 1 Room of the Saclay Linear Accelerator Laboratory, Instituto Nazionale di Fisica Nucleare Laboretori Nazioneli de Frascati, report LNF-80/39(R) (1980).

BARTEL, W. and F.W. Busser, W.R. Dix, R. Felst, D. Harms, H. Krehbiel, P. Kuhlmann, J. McElroy, J. Meyer and G. Weber, Nucl. Phys. B58, 429 (1973).

DYTMANN, S., Private Communication (1987).

GALSTER, S. and H. Klein, J. Moritz, K.H. Schmidt, D. Wegener and J. Blechwenn, Nucl. Phys. B32, 221 (1971).

HUGHES, E.B. ad T.A. Griffy, M.R. Yearian, and R. Hofstadter, Phys. Rev. B139, 458 (1965).

KROHN, V.E. and G.R. Ringo, Phys. Rev. 148, 1303 (1966).

MADEY, R. and A.R. Baldwin, P.J. Pella, J. Schambach, and R.M. Sellers, "Polarimeters for Medium-Energy Neutrons", IEEE Transactions on Nuclear Science, 36, 231 (1989).

MADISON CONVENTION, in Polarization Phenomena in Nuclear Reactions, edited by H.H. Barschall and W. Haeberli, The University of Wisconsin Press, Madison, Wisconsin (1970).

MONIZ, E.J., Phys. Rev. 184, 1154 (1969).

CEBAF Experiment Requirements

Date Submitted 10 / 30 / 89

Title & Spokesperson The Electric Form Factor of the Neutron from the $d(\vec{e},e'\vec{n})p$ Reaction — Richard Madey, Spokesman

Estimated total beam time (hours)			
Electron beam energy(s) required		1.2, 2.0, 3.0, 4.0	
Beam current(s) (μA)		100 , 25 , 50	
Total μA-hours required		, ,	
Solid target(s) material	various alignment	, ,	
Solid target(s) thickness	and calibration targets	, ,	
Cryogenic target -type and length (cm)		5 cm liquid deuterium	
Power deposition in cryogenic target (Watts)		400	
Polarized beam (y/n)		y	
Polarized target (y/n)		N	
Power deposition in polarized target		-	
Effective beam spot diameter (≥100 microns)		Diffused beam spot--to reduce hea	
Scanned beam at target (y/n)			
Dispersed beam (y/n)			

Spectrometer Requirements	***e' Arm***	***Hadron Arm*** (KSU provided)
Solid angle acceptance (msr)	few	
Momentum acceptance (FWHM %)	± 5	
Momentum resolution (FWHM %)	nominal	
Scattering angle (degrees)		
Minimum	15	
Maximum		
Scattering angle, uncertainty (mr)	1.7	
Central orbit momenta (MeV/c)		
Minimum	1000	
Maximum	4000	
Spectrometer settings, reproducibility,		
Central angle (mr)	1.7	
Central momentum (MeV/c)	1	
Particle identification requirements		
Rejection type (e.g. π^-/e^-)	π^-/e^-	
Required ratio (e.g. 10^{-3})	10^{-3}	
Traceback capability required (y/n)	y	

Position accuracy along beam (mm)	10
Luminosity range (cm^{-2} sec^{-1})	$(0.4\text{-}1.6)\times10^{38}$

Remarks: 1. Neutron polarimeter to be provided by Kent State University.
2. Shielding and movable platform for shielding and polarimeter are required from CEBAF.

Continuous Electron Beam Accelerator Facility

12000 Jefferson Avenue
Newport News, Virginia 23606
(804) 249-7100

Proposal Number: PR-89-005

Proposal Title: The Electric Form Factor of the Neutron From the d(e,e′,p)n Reaction

Spokespersons/Contact Persons: R. Madey

Proposal Status at CEBAF:

Conditional approval.

John Dirk Walecka
Scientific Director